ELSEVIER

Journal of Biomechanics 36 (2003) 1659–1668

JOURNAL OF BIOMECHANICS

www.elsevier.com/locate/jbiomech
www.JBiomech.com

Experimental evaluation of an elastic foundation model to predict contact pressures in knee replacements

Benjamin J. Fregly[a,b,c,*], Yanhong Bei[a], Mark E. Sylvester[a]

[a] Department of Mechanical & Aerospace Engineering, University of Florida, Gainesville, FL 32611, USA
[b] Department of Biomedical Engineering, University of Florida, Gainesville, FL 32611, USA
[c] Department of Orthopaedics & Rehabilitation, University of Florida, Gainesville, FL 32611, USA

Accepted 9 April 2003

Abstract

Computational wear prediction is an attractive concept for evaluating new total knee replacement designs prior to physical testing and implementation. An important hurdle to such technology is the lack of in vivo contact pressure predictions. To address this issue, this study evaluates a computationally efficient simulation approach that combines the advantages of rigid and deformable body modeling. The hybrid method uses rigid body dynamics to predict body positions and orientations and elastic foundation theory to predict contact pressures between general three-dimensional surfaces. To evaluate the method, we performed static pressure experiments with a commercial knee implant in neutral alignment using flexion angles of 0, 30, 60, and 90° and loads of 750, 1500, 2250, and 3000 N. Using manufacturer CAD geometry for the same implant, an elastic foundation model with linear or nonlinear polyethylene material properties was implemented within a commercial multibody dynamics software program. The model's ability to predict experimental peak and average contact pressures simultaneously was evaluated by performing dynamic simulations to find the static configuration. Both the linear and nonlinear material models predicted the average contact pressure data well, while only the linear material model could simultaneously predict the trends in the peak contact pressure data. This novel modeling approach is sufficiently fast and accurate to be used in design sensitivity and optimization studies of knee implant mechanics and ultimately wear.

Keywords: Dynamic modeling; Contact pressure prediction; Total knee replacements

1. Introduction

Wear remains a primary factor limiting the life span of total knee replacements (TKRs). Liberated polyethylene wear debris can initiate osteolysis (i.e., bone destruction) resulting in pain and implant loosening. Researchers currently have three basic options for studying wear: (1) Analyze implants retrieved after failure, (2) Analyze implants retrieved post-mortem, or (3) Analyze implant wear test results. Ideally, implants prone to failure would be identified before such designs are used in patients. While revision and post-mortem retrievals are valuable for studying insert damage modes (Bartel et al., 1986), they can be difficult to obtain and take years before becoming available (Harman et al., 2001). Physical wear testing is essential, and recent knee simulator designs are becoming more successful at reproducing the wear patterns observed in retrievals (Walker et al., 1997). However, a single test can cost tens of thousands of dollars and take months to run.

A computational wear model is an attractive solution to these limitations (Sathasivam and Walker, 1998). Required inputs to such a model are in vivo tibial insert surface kinematics and contact pressures. Deformable body contact analyses, such as finite element analyses (FEA) (Bartel et al., 1986, 1995; Bendjaballah et al., 1997; D'Lima et al., 2001; Périé and Hobatho, 1998; Otto et al., 2001; Rawlinson and Bartel, 2002, Sathasivam and Walker, 1998, 1999), elasticity analyses (Bartel et al., 1986; Jin et al., 1995; Rawlinson and Bartel, 2002), and elastic foundation analyses (Blankevoort et al., 1991; Li et al., 1997; Nuño and Ahmed, 2001; Pandy

*Corresponding author. Department of Mechanical & Aerospace Engineering, University of Florida, 231 MAE-A Building, PO Box 116250, Gainesville, FL 32611, USA. Tel.: +1-352-392-8157; fax: +1-352-392-7303.
E-mail address: fregly@ufl.edu (B.J. Fregly).

0021-9290/03/$ - see front matter
doi:10.1016/S0021-9290(03)00176-3

et al., 1997), can predict contact pressures but usually only under static conditions. In contrast, rigid body contact analyses using multibody dynamic simulation methods can predict knee motion efficiently (Abdel-Rahman and Hefzy, 1998; Godest et al., 2000; Piazza and Delp, 2001) but cannot predict contact pressures (Cheng et al., 1990). Dynamic FEA codes have begun to bridge the gap between these two approaches but take hours or days of CPU time to predict motion and contact pressures simultaneously (Giddings et al., 2001; Godest et al., 2002). Thus, no fast simulation approach exists to provide the required wear model inputs, making it difficult to perform design sensitivity or optimization studies of TKR wear.

This study experimentally evaluates a novel modeling approach for predicting knee implant contact pressures during a dynamic task. The approach combines the best features of the rigid and deformable body modeling methods mentioned above. It integrates traditional multibody dynamics to predict large overall motions with deformable body contact to predict contact pressures between general three-dimensional surfaces. The resulting approach is sufficiently fast computationally to perform dynamic knee simulations in minutes rather than hours or days. Static experimental contact pressure data collected from a commercial knee implant were used to evaluate the applicability and limitations of the current formulation, which uses an elastic foundation contact model with linear or nonlinear polyethylene material properties. The ability to predict static pressures is a necessary first step to predicting dynamic pressures and ultimately wear.

2. Materials and methods

2.1. Elastic contact model

An elastic foundation contact model (Johnson, 1985; also called a rigid body spring model—An et al., 1990; Blankevoort et al., 1991; Li et al., 1997) was implemented within a commercial multibody dynamics software program (Pro/MECHANICA MOTION, Parametric Technology Corporation, Waltham, MA). The contact model is a dynamic link library that can be integrated into any multibody dynamics code and uses the ACIS 3D Toolkit (Spatial Corporation, Westminster, CO) to perform geometry evaluations between general three-dimensional surfaces. The model uses a "bed of springs" scattered over the surfaces of the contacting bodies to push the surfaces apart (Johnson, 1985). The springs represent an elastic layer of known thickness covering a rigid substrate on one or both bodies, where each spring is independent from its neighbors. If both bodies possess an elastic layer of the same material, then the two layers may be treated as a single layer of combined thickness (Li et al., 1997). Layered contact is in contrast to half-space contact, where both bodies are elastic and semi-infinite. The assumption of independent springs eliminates the integral nature of contact problems, thereby greatly simplifying the analysis of conformal geometry (e.g., a sphere in a spherical cup) or nonlinear materials.

For a rigid femoral component contacting an ultra-high molecular weight polyethylene (UHMWPE) tibial insert of finite thickness, the contact pressure p for any spring can be calculated from (Johnson, 1985; An et al., 1990; Blankevoort et al., 1991)

$$p = \frac{(1-v)E(p)}{(1+v)(1-2v)h}d, \tag{1}$$

where $E(p)$ is Young's modulus of the elastic layer, which can be a nonlinear function of p, v is Poisson's ratio of the elastic layer, h is the layer thickness at the spring location, and d is the spring deflection, defined as the interpenetration of the undeformed surfaces in the direction of the local surface normal. Note that d can be computed at each instant in time given the current position and orientation of the tibial insert and femoral component. In this study, the thickness h was calculated separately for each spring as the local insert thickness in the superior–inferior direction. Springs were distributed approximately uniformly over the tibial insert contact surfaces by projecting a planar rectangular element grid onto the insert surfaces. The number of elements was adjusted manually for each simulation such that approximately 100 springs were always "active" on each contact surface at the final static position (Fig. 1a).

Given the known value for the deflection d of any spring at each instant in time, the contact pressure p for the spring can be easily calculated. For a nonlinear material model, an equation for E as a function of p (Cripton, 1993) can be substituted into Eq. (1) to produce one nonlinear equation for p (Nuño and Ahmed, 2001). Since each spring is independent of its neighbors, any standard nonlinear root-finding algorithm can solve the resulting system of nonlinear pressure equations independently. For a linear material model, Eq. (1) can be solved directly for p. The calculated pressures can then be multiplied by their corresponding areas to produce a set of point forces. Finally, these forces can be replaced with a single equivalent force and torque applied to the rigid bodies for purposes of dynamic simulation (Kane and Levinson, 1985). For comparison with the experiments, average pressure was calculated by averaging all non-zero pressures.

2.2. Parametric material model

To facilitate the use of optimization in this solution process, a parametric material model with a minimal number of parameters was developed to represent the

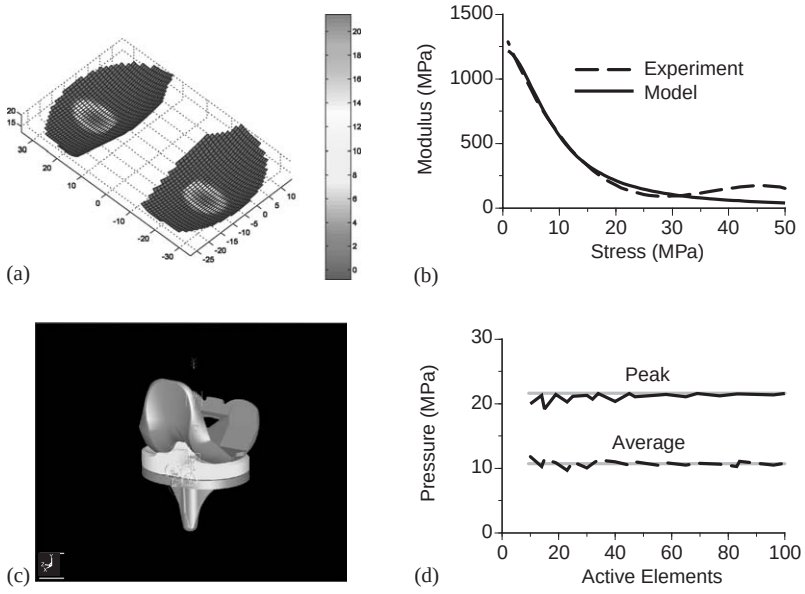

Fig. 1. Overview of materials and methods. (a) Typical three-dimensional pressure plot demonstrating the uniform distribution of springs over the tibial insert contact surfaces. (b) Comparison of the parametric nonlinear material model to experimental UHMWPE Young's modulus-stress data reported by Cripton (1993) at 23°C. (c) Multibody dynamic contact model implemented within the Pro/MECHANICA MOTION simulation environment using commercial knee implant CAD geometry. (d) Sensitivity of predicted average and peak contact pressures to the number of active elements in a contact region. Convergence to within 10% error occurs by 25 elements and 5% error by 50 elements. Assumed "true" values determined using 400 active elements per side are indicated by gray lines.

nonlinear properties of UHMWPE:

$$\varepsilon = \frac{1}{2}\varepsilon_0 \frac{\sigma}{\sigma_0} + \frac{1}{2}\varepsilon_0 \left(\frac{\sigma}{\sigma_0}\right)^n, \tag{2}$$

where ε is strain, σ is stress, and ε_0, σ_0, and n are material parameters. This is the nonlinear power-law material model discussed in Johnson (1985) but with the addition of a linear term. This model has the advantages that only three parameters are required to define a material, making the model easy to use for design sensitivity and optimization studies, and that choosing $n = 1$ produces a standard linear material model. For a given value of σ, the current value of $E = d\sigma/d\varepsilon$ for any spring can be found from

$$E = 1/\left\{\frac{1}{2}\frac{\varepsilon_0}{\sigma_0}\left[1 + n\left(\frac{\sigma}{\sigma_0}\right)^{n-1}\right]\right\}. \tag{3}$$

Eq. (3) was fit to the experimental E versus σ data reported by Cripton (1993) at 23°C and 37°C. For both temperatures, $n = 3$ provided the best fit to the experimental data (Fig 1b; $R^2 = 0.966$ at 23°C with $\varepsilon_0 = 0.0257$ and $\sigma_0 = 15.8$; $R^2 = 0.925$ at 37°C with $\varepsilon_0 = 0.0597$ and $\sigma_0 = 18.4$).

For comparison purposes, both linear ($n = 1$) and nonlinear ($n = 3$) UHMWPE material models were used in this study. For both models, ε_0 was fixed and σ_0 tuned to match the average contact pressure from the 0° flexion/3000 N experiment (see below), since the largest load would subject the material to the greatest range of pressures. The tuned parameters for the linear model were $\varepsilon_0 = 1$, $\sigma_0 = 400$, corresponding to a constant Young's modulus of 400 MPa, which is close to the value of 463 MPa recently reported by Kurtz et al. (2002). For the nonlinear model they were $\varepsilon_0 = 0.0257$, $\sigma_0 = 15.9$, very close to material parameters determined from Cripton's data at 23°C. Poisson's ratio for the polyethylene was 0.46 for both material models (Bartel et al., 1995). These tuned parameters were used to simulate the remaining 15 experimental cases (see below).

2.3. Dynamic implant model

Using this contact algorithm, a dynamic model with elastic contact was created using CAD geometry from a commercial knee implant possessing medial–lateral symmetry and a 9 mm minimum insert thickness (Fig. 1c; Optetrak B, Exactech Corporation, Gainesville, FL). To simplify the geometry evaluations and eliminate potential problems caused by seams between surface patches, medial and lateral femoral contact surfaces (four per side) were replaced with single surface approximations using Geomagic Studio (Raindrop Geomagic, Research Triangle Park, NC) and Rhinoceros (Robert McNeel & Associates, Seattle, WA) software. The tolerance between the original and approximate surfaces in the regions of contact was

measured with Geomagic Studio to be ± 0.002 mm, well within manufacturing tolerance.

The dynamic model was constructed to emulate the experimental set-up described below, which was designed to produce approximately equal contact forces, peak pressures, average pressures, and contact areas in the medial and lateral compartments. Deformable contact was permitted between the medial femoral condyle and insert surface, the lateral femoral condyle and insert surface, and the femoral cam and tibial post. A fixed force was applied vertically downward to the femoral component at the approximate point of load application in the experiments. The femoral component was connected to the tibial insert via a six degree-of-freedom (DOF) joint. Sagittal plane translations and varus–valgus rotation were free while the remaining three DOFs were fixed. The flexion angle was fixed at each of the four experimental values. To account for small variations in experimental positioning (Liau et al., 1999), an optimization was performed for each flexion angle to find the medial–lateral translation and internal–external rotation that best matched the experimental peak and average contact pressures simultaneously. This procedure was performed only for the 3000 N load, with the resulting translation and rotation being used for the remaining three loads. The optimized position was the same for both material models. Maximum medial–lateral translation was 0.35 mm and maximum axial rotation was 1.5°, well within the expected experimental variations.

With any numerical approach involving elements, an important issue is the number of elements required to produce an accurate solution. To address this issue, we performed a global sensitivity study to investigate the convergence of the peak and average contact pressures as a function of the number of active springs. The sensitivity study was performed using the 0° flexion/3000 N load case. Assuming the "true" solution corresponded to 400 active elements per side, peak and average contact pressure were within 10% error by only 25 active elements and 5% error by 50 active elements (Fig. 1d). Thus, 100 active elements per side were more than accurate enough for comparison with experimental data.

With the relative component positioning and accuracy requirements established, a global sensitivity study was performed for each flexion angle to predict the variation in peak and average contact pressure with load. For each load, the sensitivity study performed a forward dynamic simulation using implicit integration with numerical damping (rather than physical damping) to cause the components to settle together into a static configuration (Fig. 2). Mass and inertia of the femoral component were computed from its geometry assuming uniform density. Each dynamic simulation was terminated when all translational and rotational accelerations were less than a small user-defined tolerance (1e-5 mm/s^2 and rad/s^2 in our simulations). Typical computation time for a single dynamic simulation with 100 active elements per side was less than 30 s on a 1.2 GHz Pentium III-M laptop computer. In all, 16 experimental cases (four flexion angles with four loads per flexion angle; see below) were predicted by the sensitivity studies. All optimization and sensitivity studies were performed with Pro/MECHANICA MOTION's built-in design study capabilities.

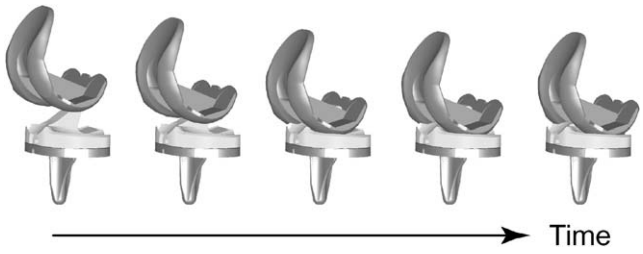

Fig. 2. Visualization of example dynamic simulation used to settle the femoral component onto the tibial insert. Time flows from left (initial configuration) to right (final static configuration). The dynamic simulation is terminated when all translational and rotational accelerations are less than a small user-defined tolerance.

2.4. Contact pressure experiments

A commercial knee implant identical to the CAD model described above was used in the experiments (Fig. 3a). Fixturing allowed the femoral component to be positioned at flexion angles of 0, 30, 60, and 90° relative to the tibial component. The femoral component was connected to the ram of an MTS servohydraulic test machine via a pin joint that allowed varus–valgus rotation, thereby permitting equilibration of the frontal plane contact moment (Harris et al., 1999). A lockable slider joint was located above this pin joint to allow medial–lateral positioning of the vertical load axis above the center of the femoral component (Harris et al., 1999). The tibial component was mounted to the top of a tilt table with lockable varus–valgus rotation and horizontal plane translations. To facilitate comparison with the model, the knee was tested in neutral alignment with the DOFs adjusted via trial and error until approximately equal contact force, peak pressure, average pressure, and contact area were obtained in the medial and lateral compartments.

To provide a wide range of conditions for evaluating the model, 16 experimental cases were used, composed of all possible combinations of four flexion angles (0, 30, 60, and 90°) and four loads (750, 1500, 2250, and 3000 N). The loads were representative of approximately one to four times body weight. All tests were performed at 23°C, and three separate trials were performed for each case. Contact pressure and area data were collected

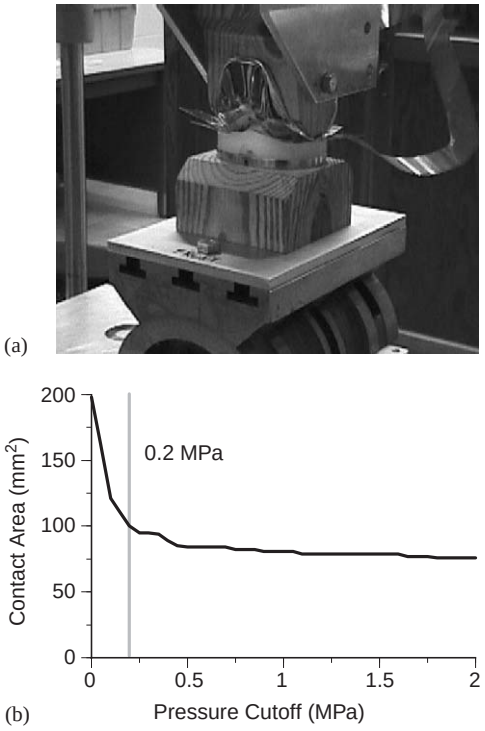

Fig. 3. (a) Experimental contact pressure measurements made on the same implant using a Tekscan K-Scan pressure measuring system and a servohydraulic test machine. (b) Sensitivity of experimental contact area to the pressure cut-off value selected for the Tekscan sensor. The change in contact area stabilizes by about 0.2 MPa, as indicated by the gray line.

from the medial and lateral compartments of the implant using a Tekscan K-Scan pressure measuring system with a fresh sensor (Harris et al., 1999). Though the sensor will affect the pressure measurements (Wu et al., 1998), the effect is expected to be much less than in natural joints where the sensor is stiffer than the contacting surfaces. Results from both compartments were averaged (total of six measurements) to produce mean and standard deviation data for evaluation of model predictions.

Four issues related to the Tekscan sensor required special attention. The first was the development of an accurate calibration procedure. Since the K-Scan sensor has been shown to exhibit significant calibration drift over time (Otto et al., 1999), each experimental trial was self-calibrated. Ramp loads from 20% to 100% of desired load were applied over 5 s, and these two points were used to perform the two-point calibration procedure recommended by the manufacturer. The two loads required for post-calibration were measured during each trial by an in-line load cell. Thus, the total load measured by the sensor always matched the load applied by the MTS machine. Because each trial was calibrated using load cell measurements from the same trial, trial-to-trial calibration drift was eliminated.

The second issue was determination of an appropriate pressure cut-off value. Due to the moderately conformal nature of the knee design tested, the sensor "crinkled" slightly during the experiments (Lewis, 1998). These crinkles introduce erroneous contact pressures on sensels outside the true contact area, making it necessary to determine a pressure below which all measured sensel pressures are set to zero. To determine this cut-off, we plotted the experimentally measured contact area for the 0° flexion/1500 N load case using pressure cut-off values ranging from 0 to 2 MPa (Fig. 3b). While changing the cut-off had little effect on the measured contact force or peak pressure, it had a dramatic effect on the measured contact area and hence average pressure. In particular, changing the pressure cut-off from 0 to 0.2 MPa resulted in a 50% drop in contact area. Since little additional drop in area occurred beyond 0.2 MPa, we chose this as our cut-off. Average experimental pressures were therefore calculated by ignoring all sensels with pressures below 0.2 MPa.

The third issue was the methodology used to calculate peak pressures. Because peak pressure can be sensitive to measurements from a single sensel, this quantity was determined using two approaches. The first used the maximum pressure recorded by a single sensel. The second applied the built-in averaging function available in the Tekscan software prior to determining the sensel with maximum pressure. This function performs weighted averaging of each sensel with its eight neighbors, which eliminates local "hot spots" from a single sensel due to sensor crinkling, small surface imperfections, or non-uniform response from the sensels. Since averaging reduces peak pressure measurements, results without averaging can be viewed as an upper bound on the peak pressure and results with averaging as a lower bound.

The final issue was estimation of pressure measurement errors due to sensor discretization. The K-Scan sensor measures pressures on discrete sensels with an area of 1.61 mm^2. Thus, both peak and average pressure measurements will be influenced by the sensel size. To estimate the magnitude of discretization errors, a theoretical power law relationship was used (see Fregly and Sawyer, 2003 for details). This relationship estimates peak and average pressure errors as a function of a non-dimensional area variable, defined as the ratio of the number of perimeter sensels in the contact patch to the total number of sensels with pressure. At 0° flexion, calculation of this non-dimensional variable from the active Tekscan sensels indicated errors on the order of 1–2% for peak and 3–6% for average pressure. Though errors will be slightly larger at 90° where the contact area is smaller, these errors were deemed to be sufficiently small not to hinder comparison with model predictions.

3. Results

The linear and nonlinear contact models were evaluated by their ability to match experimental peak and average contact pressures simultaneously. Matching both is necessary for the predicted pressure distribution to match the experiments. Contact force comparisons are not reported since the force is always matched exactly at the final static configuration. Contact area comparisons are not reported since the area follows similar, but inverted, trends to the average pressure (e.g., a slightly high predicted average pressure means a slightly low predicted contact area).

The linear material model predicted the experimental data more closely than did the nonlinear material model, with mean, standard deviation and RMS errors typically being two to three times smaller for the linear model (Table 1). Both models tracked the average contact pressure well, though the linear model tracked it better (Fig. 4a). Since the contact force was always matched exactly, the contact area was also predicted well by both material models. In contrast, only the linear model tracked the peak pressure well. The peak pressure predicted by the linear model was generally between the two experimental measurements (with and without averaging), whereas that predicted by the nonlinear model was consistently below the two experimental measurements except at 750 N (Fig. 4b). Both models predicted posterior cam contact only at 90°, which was consistent with the experiments.

Table 1
Mean, standard deviation (SD), and root-mean-square (RMS) errors in predicted peak and average contact pressures for the 16 experimental cases using the linear and nonlinear material models

Errors (MPa)		Linear model	Nonlinear model
Peak pressure without averaging	Mean	−2.2	−6.7
	SD	1.2	3.6
	RMS	2.5	7.5
Peak pressure with averaging	Mean	2.0	−2.5
	SD	1.4	2.7
	RMS	2.4	3.6
Average pressure	Mean	0.31	0.56
	SD	0.49	1.1
	RMS	0.57	1.2

Peak pressure was measured experimentally with and without averaging of neighboring sensels on the pressure sensor.

4. Discussion

4.1. Contact model accuracy

This study experimentally evaluates a hybrid rigid-deformable dynamic modeling approach for predicting contact pressures in total knee replacements. Though the dynamic simulations were used to predict final static configurations, the evaluation validates the computational efficiency of the approach compared to dynamic finite element methods. It also validates the accuracy of the approach for predicting static contact pressures with a single set of material parameters, which is an essential first step toward predicting dynamic contact pressures and eventually wear. Overall, these findings indicate that this novel modeling approach is well suited to sensitivity and optimization studies of knee implant designs.

An important issue affecting contact model accuracy is the choice of material model. Some finite element studies of knee replacements have used nonlinear UHMWPE material models (Bartel et al., 1995; D'Lima et al., 2001; Godest et al., 2002; Otto et al., 2001; Rawlinson and Bartel, 2002) while others have used linear material models (Bartel et al., 1986; Sathasivam and Walker, 1998, 1999). We are unaware of a previous study that has performed a thorough contact pressure comparison between model and experiments using actual implant geometry to validate either material model. At least one other study performed at 23°C found that a linear material model with a Young's modulus of 500 MPa provided the best match to experimental contact area data measured using loads between 500 and 2500 N (Stewart et al., 1995). In those experiments, a spherical glass indenter contacted a thick, wide UHMWPE block that approximated a half-space, with contact area predictions being made with a Hertz contact model. A more recent study measured Young's modulus of UHMWPE to be 463 MPa using a miniature specimen shear punch test (Kurtz et al., 2002). For an elastic foundation contact model, since pressures on surrounding elements do not contribute to the deformation of an element, a slightly lower value of Young's modulus is needed to produce the same total deformation. This explains the best-fit Young's modulus of 400 MPa found in our study.

4.2. Contact model advantages

As with any engineering model, the proposed dynamic contact model has its advantages and limitations. The primary advantages of the elastic foundation contact model are its simplicity and versatility. Since each spring is treated as independent, more computationally intensive coupled contact solutions involving either quadratic programming (Conry and Seirig, 1971; Kalker and Van Randen, 1972) or repeated linear system solution (Singh and Paul, 1974) are not needed. This makes the model ideal for incorporation into a multibody dynamic simulation framework. The independent

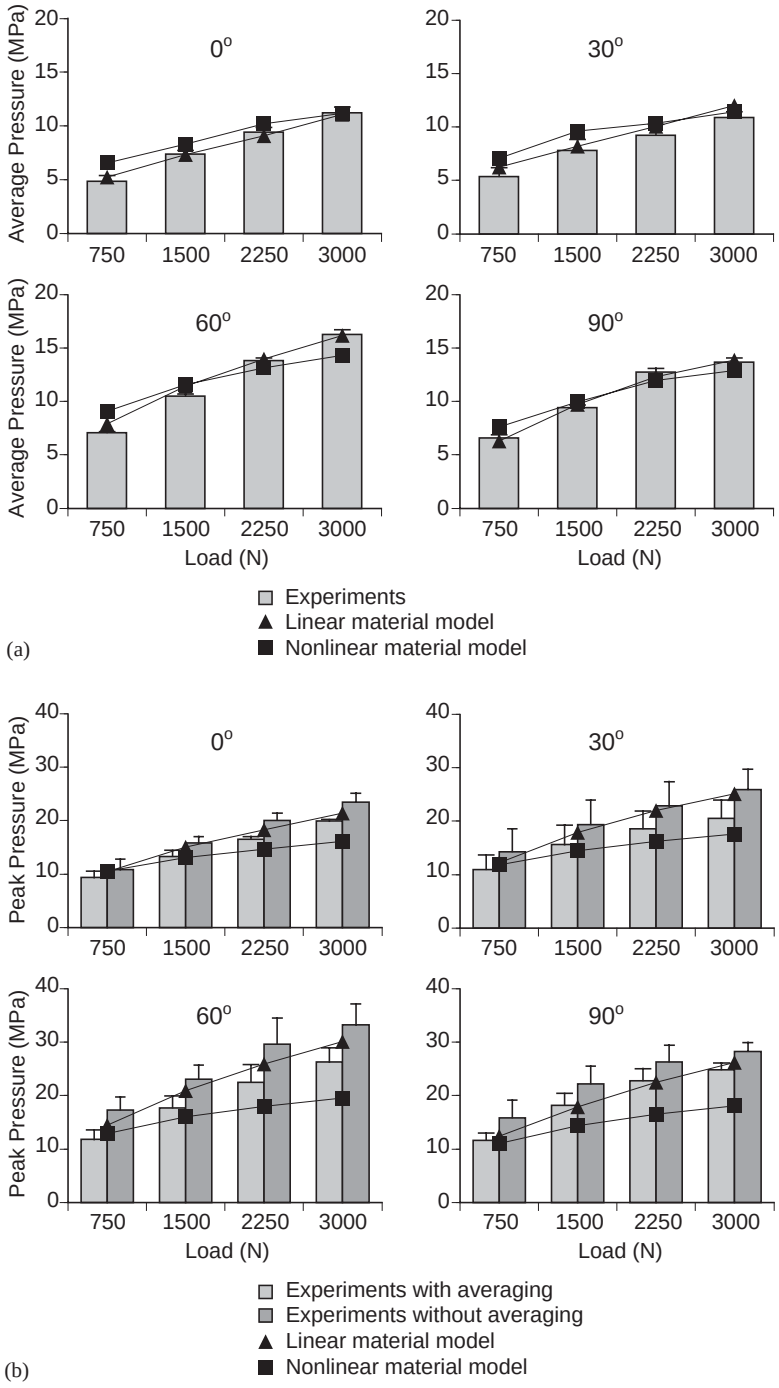

Fig. 4. Comparison between experimental and predicted (a) average and (b) peak contact pressures for all possible combinations of four flexion angles (0, 30, 60, and 90°) and four loads (750, 1500, 2250, and 3000 N). Predictions were made with a single contact model using linear (triangle symbols) and nonlinear (square symbols) UHMWPE material models. Experimental peak contact pressure measurements were made with and without averaging of neighboring sensels. Error bars on experimental data indicate ± 1 standard deviation.

nature of the springs also makes it easy to incorporate nonlinear material models into the formulation as described above. An elastic–plastic material model could be incorporated as well by following a solution process similar to the nonlinear material model. In addition, the formulation accounts for layered contact between bodies of finite and variable thickness and breadth, and conformal contact involving non-planar contact patches. Both of these features are limitations in elastic half-space contact models (Johnson, 1985). Because conformity is not an issue, the current contact model will be applicable to more or less conformal knee

implant designs than the one used here, as well as to rotating platform designs

Another advantage of this computational framework is that it is not restricted to the elastic foundation contact model evaluated here. Within the same framework, we have also implemented an elastic half-space contact model (Conry and Seirig, 1971; Kalker and Van Randen, 1972) with modifications to account for conformal contact (Paul and Hashemi, 1981). Currently, this model cannot handle layered contact, contact patches with dimensions comparable to the contacting bodies, or nonlinear materials. However, unlike the elastic foundation model, it accounts for how pressure applied at one location produces deformations at all locations. Data from this contact model are not presented here since a single value of Young's modulus could not be found that matched the experimental pressures for all loads and flexion angles. Nonetheless, this model demonstrates that more complicated contact models can easily be implemented within the same framework to address limitations in the elastic foundation model discovered through future experimental evaluation.

Previous studies have also used commercial multibody dynamics codes to simulate contact conditions in knee replacements. Similar to this study, the elastic contact model developed for ADAMS (MSC Software, Santa Ana, CA) uses discrete compressive springs on the surfaces of the contacting bodies. This model has been used to simulate stability tests (McGuan et al., 1998), knee simulator machine motions (Rullkoetter et al., 1999), and cam engagement in posterior-stabilized knees (Metzger et al., 2001). However, it predicts only contact forces, not contact pressures, and uses tessellated surface approximations that can cause force discontinuities (Puse and Laursen, 2002) that slow numerical integration. Pro/MECHANICA MOTION's built-in elastic contact model uses either a Hertz formulation for approximately quadratic surfaces or an elastic half-space boundary element formulation for general surfaces. This model has been used to simulate contact pressure as a function of flexion angle (Fregly, 1999) and peak contact pressure sensitivity to femoral component malrotation (Fregly, 2000). While the use of the actual surface geometry reduces contact force discontinuities, such half-space formulations have significant limitations as discussed above. Neither of these contact models has been used to predict experimental pressure data as done here.

4.3. Contact model limitations

Several important limitations are also present in the current formulation. First, the contact model is quasi-static and does not account for viscoelasticity (Waldman and Bryant, 1997). A viscoelastic contact model would require adding states to keep track of the deformation of each element, which would make the contact calculations more complicated. Alternatively, if the elastic parameters are tuned to match dynamic contact pressure data collected at a physiological loading rate and temperature, an equivalent set of linear material parameters could be chosen to approximate the viscoelastic situation for those loading conditions. Second, the model does not account for how pressure applied at one location produces deformations at all locations. However, this was not a serious limitation for matching our experimental data. Third, the model provides predictive information on contact pressures but not surface tensile stresses or sub-surface stresses. While the model would be useful for wear predictions made from contact pressure and kinematic inputs, predictions involving sub-surface stresses would require finite element analyses (Sathasivam and Walker, 1998). Fourth, the current model does not account for friction (Sathasivam and Walker, 1997). However, since local slip velocity information is available for each element, a Coulomb friction model can easily be added on an element-by-element basis as a reasonable approximation (Johnson, 1985). Fifth, the model has only been evaluated for a knee implant, but given the versatility of the approach, it would likely be applicable to other artificial joints as well (An et al., 1990; Li et al., 1997; Genda et al., 2001).

The applicability of the linear material model to larger peak contact pressures requires further investigation. The force applied to each side was a maximum of 1500 N. During gait, it is possible that the entire load could be borne on one condyle (Stiehl et al., 1999). At 1500 N per condyle, the peak contact pressure in our experiments was between 25 and 35 MPa (Fig. 4b). Assuming polyethylene has a yield stress of 14 MPa (Bartel et al., 1995), yielding will be initiated below the surface when the peak contact pressure reaches approximately 1.6 times the yield stress (Johnson, 1985) or about 22.5 MPa. Thus, significant plastic deformation may not have occurred over the course of the experiments. This hypothesis is supported by the model's prediction of only 4% maximum strain, making it less surprising that the linear material model worked so well. Implementation of an elastic–plastic contact model, as described above, may therefore be required to model higher contact pressures.

Acknowledgements

This study was funded in part by NIH grant 1 R03 LM07332-01 from the National Library of Medicine and by Exactech Corporation. We thank Andy Rapoff and Wes Johnson for assistance with preliminary experimental fixturing and use of the MTS machine used in this study, Kelly Rooney for assistance with

Tekscan data processing, Mike Sherman for assistance with Pro/MECHANICA MOTION custom load implementation, and Scott Banks for helpful comments on the manuscript.

References

Abdel-Rahman, E.M., Hefzy, M.S., 1998. Three-dimensional dynamic behavior of the human knee joint under impact loading. Medical Engineering and Physics 20, 276–290.

An, K.N., Himenso, S., Tsumura, H., Kawai, T., Chao, E.Y.S., 1990. Pressure distribution on articular surfaces: application to joint stability analysis. Journal of Biomechanics 23, 1013–1020.

Bartel, D.L., Bicknell, V.L., Wright, T.M., 1986. The effect of conformity, thickness, and material on stresses in ultra-high molecular weight components for total joint replacement. Journal of Bone and Joint Surgery 68-A, 1041–1051.

Bartel, D.L., Rawlinson, J.J., Burstein, A.H., Ranawat, C.S., Flynn, W.F., 1995. Stresses in polyethylene components of contemporary total knee replacements. Clinical Orthopaedics and Related Research 317, 76–82.

Bendjaballah, M.Z., Shirazi-Adl, A., Zukor, D.J., 1997. Finite element analysis of human knee joint in varus–valgus. Clinical Biomechanics 12, 139–148.

Blankevoort, L., Kuiper, J.H., Huiskes, R., Grootenboer, H.J., 1991. Articular contact in a three-dimensional model of the knee. Journal of Biomechanics 24, 1019–1031.

Cheng, R.C.-K., Brown, T.D., Andrews, J.G., 1990. Non-uniqueness of the bicompartmental contact force solution in a lumped parameter mathematical model of the knee. Journal of Biomechanics 23, 353–355.

Conry, T.F., Seirig, A., 1971. A mathematical programming method for design of elastic bodies in contact. Journal of Applied Mechanics 38, 387–392.

Cripton, P.A., 1993. Compressive characterization of ultra-high molecular weight polyethylene with applications to contact stress analysis of total knee replacements. Master of Science Thesis, Queen's University, Kingston, Ontario.

D'Lima, D.D., Chen, P.C., Colwell, C.W., 2001. Polyethylene contact stresses, articular congruity, and knee alignment. Clinical Orthopaedics and Related Research 392, 232–238.

Fregly, B.J., 1999. A three-dimensional compliant contact model for dynamic simulation of total knee replacements. In: Proceedings of the VIIth International Symposium on Computer Simulation in Biomechanics. University of Calgary, Calgary, Canada, 10–13.

Fregly, B.J., 2000. Effect of femoral component malrotation on contact stress in total knee replacements. In: Proceedings of the 24th Annual Meeting of the American Society of Biomechanics. University of Illinois at Chicago, Chicago, IL, 101–102.

Fregly, B.J., Sawyer, W.G., 2003. Estimation of decretization errors in contact pressure measurements. Journal of Biomechanics 30, 177–184.

Genda, E., Iwasaki, N., Li, G., MacWilliams, B.A., Barrance, P.J., Chao, E.Y.S., 2001. Normal hip joint contact pressure distribution in single-leg standing-effect of gender and anatomic parameters. Journal of Biomechanics 34, 895–905.

Giddings, V.L., Kurtz, S.M., Edidin, A.A., 2001. Total knee replacement polyethylene stresses during loading in a knee simulator. Journal of Tribology 123, 842–847.

Godest, A.C., Meaugonin, M., Haug, E., Taylor, M., Gregson, P.J., 2002. Simulation of a knee joint replacement during a gait cycle using explicit finite element analysis. Journal of Biomechanics 35, 267–276.

Godest, A.C., Simonis de Cloke, C., Taylor, M., Gregson, P.J., Keane, A.J., Sathasivan, S., Walker, P.S., 2000. A computational model for the prediction of total knee replacement kinematics in the sagittal plane. Journal of Biomechanics 33, 435–442.

Harman, M.K., Banks, S.A., Hodge, W.A., 2001. Polyethylene damage and knee kinematics after total knee arthroplasty. Clinical Orthopaedics and Related Research 392, 383–393.

Harris, M.L., Morberg, P., Bruce, W.J.M., Walsh, W.R., 1999. An improved method for measuring tibiofemoral contact areas in total knee arthroplasty: a comparison of K-scan sensor and Fuji film. Journal of Biomechanics 32, 951–958.

Jin, Z.M., Dowson, D., Fisher, J., 1995. Contact pressure prediction in total knee joint replacements.: Part 1: general elasticity solution for elliptical layered contacts. Proceedings of the Institution of Mechanical Engineers Part H 209, 1–8.

Johnson, K.L., 1985. Contact Mechanics. Cambridge University Press, Cambridge.

Kalker, J.J., Van Randen, Y., 1972. A minimum principle for frictionless elastic contact with application to non-Hertzian half-space contact problems. Journal of Engineering Mathematics 6, 193–206.

Kane, T.R., Levinson, D.A., 1985. Dynamics: Theory and Applications. McGraw-Hill, New York.

Kurtz, S.M., Jewett, C.W., Bergström, J.S., Foulds, J.R., Edidin, A.A., 2002. Miniature specimen shear punch test for UHMWPE used in total joint replacements. Biomatierals 23, 1907–1919.

Lewis, G., 1998. Contact stress at articular surfaces in total joint replacements. Part I: experimental methods. Bio-Medical Materials and Engineering 8, 91–110.

Li, G., Sakamoto, M., Chao, E.Y.S., 1997. A comparison of different methods in predicting static pressure distribution in articulating joints. Journal of Biomechanics 30, 635–638.

Liau, J.-J., Cheng, C.-K., Huang, C.-H., Lee, Y.-M., Chueh, S.-C., Lo, W.-H., 1999. The influence of contact alignment of the tibofemoral joint of the prosthesis in in vitro biomechanical testing. Clinical Biomechanics 14, 717–721.

McGuan, S., Jasty, M.,Kaufman, M., 1998. Total knee system performance measurement through computerized intrinsic stability testing. In: Proceedings of the 65th Annual Meeting of the American Academy of Orthopaedic Surgeons. New Orleans, LA.

Metzger, R., Lombardi, A.V., Mallory, T.H., Fada, R.A., Hartman, J.F., Adamsn, J.B., McGuan, S.P., 2001. Late versus early engagement of posterior stabilized prostheses: effect on extensor moment arm and resultant extensor loads. In: Proceedings of the 47th Annual Meeting of the Orthopaedic Research Society. San Francisco, CA.

Nuño, N., Ahmed, A.M., 2001. Sagittal profile of the femoral condyles and its application to femorotibial contact analysis. Journal of Biomechanical Engineering 123, 18–26.

Otto, J.K., Brown, T.D., Callaghan, J.J., 1999. Static and dynamic response of a multiplexed-array piezoresistive contact sensor. Experimental Mechanics 39, 317–323.

Otto, J.K., Callaghan, J.J., Brown, T.D., 2001. Mobility and contact mechanics of a rotating platform total knee replacement. Clinical Orthopaedics and Related Research 392, 24–37.

Pandy, M.G., Sasaki, K., Kim, S., 1997. A three-dimensional musculoskeletal model of the human knee joint. Part 1: theoretical construction. Computer Methods in Biomechanics and Biomedical Engineering 1, 87–108.

Paul, B., Hashemi, J., 1981. Contact pressures on closely conforming elastic bodies. Journal of Applied Mechanics 48, 543–548.

Périé, D., Hobatho, M.C., 1998. In vivo determination of contact areas and pressure of the femorotibial joint using non-linear finite element analysis. Clinical Biomechanics 13, 394–402.

Piazza, S.J., Delp, S.L., 2001. Three-dimensional dynamic simulation of total knee replacement motion during a step-up task. Journal of Biomechanical Engineering 123, 599–606.

Puse, M.A., Laursen, T.A., 2002. A 3D contact smoothing method using Gregory patches. International Journal for Numerical Methods in Engineering 54, 1161–1194.

Rawlinson, J.J., Bartel, D.L., 2002. Flat medial–lateral conformity in total knee replacements does not minimize contact stress. Journal of Biomechanics 35, 27–34.

Rullkoetter, P.J., McGuan, S., Maletsky, L.P., 1999. Development and verification of a virtual knee simulator for TKR evaluation. In: Proceedings of the 45th Annual Meeting of the Orthopaedic Research Society. Anaheim, CA.

Sathasivam, S., Walker, P.S., 1997. A computer model with surface friction for the prediction of total knee kinematics. Journal of Biomechanics 30, 177–184.

Sathasivam, S., Walker, P.S., 1998. Computer model to predict subsurface damge in tibial inserts of total knees. Journal of Orthopaedic Research 16, 564–571.

Sathasivam, S., Walker, P.S., 1999. The conflicting requirements of laxity and conformity in total knee replacements. Journal of Biomechanics 32, 239–247.

Singh, K.P., Paul, B., 1974. Numerical solution of non-Hertzian elastic contact problems. Journal of Applied Mechanics, 484–490.

Stewart, T., Jin, Z.M., Shaw, D., Auger, D.D., Stone, M., Fisher, J., 1995. Experimental and theoretical study of the contact mechanics of five total knee joint replacements. Proceedings of the Institution of Mechanical Engineers Part H 209, 225–231.

Stiehl, J.B., Dennis, D.A., Komistek, R.D., Crane, H.S., 1999. In vivo determination of condylar lift-off and screw-home in a mobile-bearing total knee arthroplasty. Journal of Arthroplasty 14, 293–299.

Waldman, S.D., Bryant, J.T., 1997. Dynamic contact stress and rolling resistance model for total knee arthroplasties. Journal of Biomechanical Engineering 119, 254–260.

Walker, P.S., Blunn, G.W., Broome, D.R., Perry, J., Watkins, A., Sathasivam, S., Dewar, M.E., Paul, J.P., 1997. A knee simulating machine for performance evaluation of total knee replacements. Journal of Biomechanics 30, 83–89.

Wu, J.Z., Herzog, W., Epstein, M., 1998. Effects of inserting a pressensor film into articular joints on the actual contact mechanics. Journal of Biomechanical Engineering 120, 655–659.